Catalysis Today 147S (2009) S94–S98

Contents lists available at ScienceDirect

Catalysis Today

journal homepage: www.elsevier.com/locate/cattod

In search for active non-precious metal catalyst for VOC combustion Evaluation of plasma deposited Co and Co/Cu oxide catalysts on metallic structured carriers

Joanna Lojewska [a,*], Andrzej Kolodziej [b], Ryszard Kapica [c], Arkadiusz Knapik [a], Jacek Tyczkowski [c]

[a] Jagiellonian University, Faculty of Chemistry, Ingardena 3, 30-060 Kraków, Poland
[b] Institute of Chemical Engineering of the Polish Academy of Sciences, Bałtycka 5, 44-100 Gliwice, Poland
[c] Technical University of Lodz, Faculty of Process and Environmental Engineering, Wólczańska 213, 90-924 Łódź, Poland

ARTICLE INFO

Article history:
Available online 30 July 2009

Keywords:
VOC combustion
Combustion kinetics
Wire gauzes
Structured reactor
CoCu catalyst

ABSTRACT

The study is devoted to the evaluation of the cobalt and copper doped cobalt catalysts deposited on the structured carriers for VOC combustion. The catalysts have been tested in *n*-hexane oxidation in the jet-stirred gradientless reactor at various temperatures. As the reactor has occurred not to provide sufficient mixing conditions a model has been proposed which allowed to discriminate between external mass transport phenomena and the intrinsic kinetics. The values of the activation energy found for cobalt catalysts were higher than usually reported in the literature indicating the necessity of lab-to-lab normalisation of the results. The best performance in *n*-hexane combustion was observed for the copper doped cobalt catalyst on the wire gauze carrier which showed the lowest light-off temperature (220 °C) and the highest reaction rate with activation energy (111 kJ/mol) comparable to other cobalt catalysts studied.

1. Introduction

Structured metallic carriers of short channels have proved to be an efficient alternative for ceramic monoliths in catalytic combustion processes [1–3]. Their advantageous performance is mainly a consequence of highly increased mass transport properties. Another challenge for combustion is non-precious metal catalyst whose activity would be sufficiently high to match the enhanced mass transport to give high unlimited overall reaction rate. For this particular process the catalyst should be very flexible both in terms of temperature behaviour and a variety of compounds to deal with. Of high demand are materials which are insensitive to sintering or decomposition at possibly high temperatures, but at the same time able to initiate reaction at low temperatures. VOCs is a term broad enough to include a huge number of hydrocarbons and their oxygenates which are difficult to convert for the thermodynamic and kinetic reasons.

The noble metal catalysts are hard to compete in activity but they are vulnerable to coking [4] and sintering above 1000 °C [5]. Metal oxide spinel seems to have an interesting structure from the point of view of the catalytic redox properties. The electron transfer is secured by two oxidation states of metal and open tetrahedral voids with lower oxidation number in the oxygen crystal sublattice. Cobalt spinel in both pure and bimetallic form has been studied for its low cost, good activity [6–8] and low temperature of combustion of VOC oxygenates [6] as well as soot particles [9–11]. The spinel structure is also the most thermodynamically stable among the cobalt oxides but at temperatures below 700 °C [12–14] which in practice excludes its application for other than VOC combustion processes.

In this study we focus on the combustion performance of the cobalt catalyst both in pure and bimetallic form deposited on wire gauze carriers with non-equilibrium plasma technique (NEP). According to our previous results NEP shows a great deal of promise to meet the requirements stated above for the combustion catalysts [3,15]. The NEP method has been optimised for cobalt catalysts which deposited on wire gauzes occurred to bear a competition with platinum supported catalysts in but initiated the reaction at higher temperature (350 °C) [16–18]. For this reason and in order to stabilise the cobalt oxide structure, the cobalt catalysts were modified by doping with copper.

2. Experimental

A series of the catalysts differing in catalyst amount, composition and preparation conditions were obtained in a plasma reactor from the catalyst precursors: Co(I)-cyclopentadienyldicarbonyl

* Corresponding author at: Jagiellonian University, Faculty of Chemistry, Ingardena 3, 30-060 Kraków, Poland.
E-mail address: lojewska@chemia.uj.edu.pl (J. Lojewska).

0920-5861/$ – see front matter © 2009 Elsevier B.V. All rights reserved.
doi:10.1016/j.cattod.2009.07.021

Nomenclature

A	catalyst external surface area (m^2)
B	constant, Eq. (14)
C_A, C_{AS},	reagent concentration: in gas stream; on catalyst surface ($kmol/m^3$)
d	characteristic dimension (m)
D_A	kinematic diffusivity (m^2/s)
E_{app}, E_A	apparent, true activation energy, respectively (kJ/mol)
G	mass stream (kg/s)
k_{app}, k_r	apparent, true kinetic rate constant, respectively (m/s)
$k_{app,\infty}$, $k_{r,\infty}$	apparent, true pre-exponential constants (Arrhenius equation), respectively (m/s)
k_C	mass transfer coefficient (m/s)
r_A	kinetic rate ($kmol/m^2/s$)
R	gas constant (J/K/mol)
Re	Reynolds number
Sc	Schmidt number
Sh	Sherwood number
T	temperature (K)
V^*	volumetric flow (m^3/s)
w	gas velocity (m/s)

Greek letters

ε	void volume
η	dynamic viscosity (Pa s)
ρ	density (kg/m^3)

Subscripts

0, 1	denotes reactor inlet and outlet, respectively

and Cu(II)-acetylacetate introduced to the flow of the carrier gas: argon and/or oxygen. The thin films were deposited on the steel sheets (00H20J5, Strzemieszyce, Poland) and knitted wire gauzes made of the same steel (17.5 mesh/in., wire diameter d = 0.1 mm). The steel contains: Cr: 20.37%, Al: 5.17% and also Mn: 0.25%, Ni: 0.16%, Cu: 0.034%, Co: 0.021%.

Prior to plasma treatment the carriers were precalcined at 900 °C for 48 h to obtain a segregated layer of alumina on top of the steel sheet on which the catalyst precursors adhere [17,18]. The details on the preparation conditions and on the catalyst composition are included in Table 1. The precalcined (air, 550 °C, 24 h) cobalt foil (+99.99%, Aldrich) was used as a reference sample for kinetic tests.

The catalysts obtained were tested in *n*-hexane oxidation in a gradientless reactor CSTR purchased for this kind of experiments (Microberty, AutoClave Engineers). The reactor [19] is built of a basket container to hold the catalysts samples and a head with a rotor of controllable speed to mix a gas residing in the reactor. The design of the geometry of the reactor internal enables rapid circulation of the gas to approach ideal CSTR conditions. The reactor operated in a continuous flow of reactants at atmospheric pressure. To obtain reproducible results of catalytic tests the catalysts on steel sheets were cut into pieces to give the total surface area in the range of 10–20 cm^2. A description of the analytical and gas supplying systems can be found in [17,18]. Prior to kinetic tests the samples were activated at 350 °C for 1 h in oxygen. During temperature screening experiments the *n*-hexane concentration of 0.75 mol% was used at a total flow rate of reactants 100 cm^3/min and in the 100–550 °C temperature range.

The reaction rate was calculated from a mass balance for an ideal CSTR packed with supported catalyst of the total external surface area A:

$$-r_A = \frac{C_{A0} - C_{A1}}{A} V^* \quad (1)$$

here, the reaction rate is referred to the catalyst external surface area A, C_{A0} and C_{A1} are the hydrocarbon concentrations on the reactor inlet and outlet, respectively, and V^* is the volumetric flow through the gradientless reactor. The activation energy and infinite rate constant (pre-exponential factor) were calculated from the Arrhenius equation assuming first-order reaction kinetics and low conversion (<40%).

3. Kinetic results

The results of the temperature screening of the catalysts obtained for both the catalysts types deposited on wire gauzes and on the steel sheets are presented in Figs. 1 and 2, respectively. In addition to direct temperature dependence presented in Figs. 1A and 2A the data conversion into Arrhenius plots is presented in Figs. 1B and 2B.

The catalysts can be evaluated using several criteria such as overall reaction rate, infinite rate constant, activation energy and temperature of the reaction initiation provided that the impact of the mass transport on the observed overall reaction rate is known or negligible. Even in the jet-stirred reactor we observe the reaction rate slowing down at higher temperature for the gauze samples as in Fig. 1B and in the whole used temperature range for the sheet samples as in Fig. 2B. The question arises to which extent mass transport influences the kinetic results in the reactor used by us.

The values of the derived kinetic parameters for reactor modelling will thus depend on the temperature range chosen more or less arbitrary for fitting of the Arrhenius function. These have been calculated for the lower temperature ranges as shown in Figs. 1B and 2B and presented in Table 2 and as $k_{app,\infty}$ and E_{app}. The

Table 1
Preparation conditions and composition of the cobalt catalyst obtained with NEP technique.

Sample name	Carrier type	Carrier precalcination	Conditions of NEP deposition			Deposited Co surface concentration[a]
			Gas phase composition		Time (h)	Co (mg/cm^2)
Cu/g	CrAl gauze	48 h, 900 °C	20 mol% O_2, 80 mol% Ar	Cu(II)-acetylacetate	2	–
CoCu/g				Co(I)-cyclopentadienyldicarbonyl Cu(II)-acetylacetate	2	0.90
Co2/g				Co(I)-cyclopentadienyldicarbonyl	2	0.91
Co1/g					1	0.45
Co2/s	CrAl sheet				2	0.95
Co1/s					1	0.47
Co/f	Co foil	24 h, 550 °C	–	–	–	–

[a] Estimated from the measurements of the layer thickness from ellipsometric measurements [14], related to total surface geometrical area of a carrier.

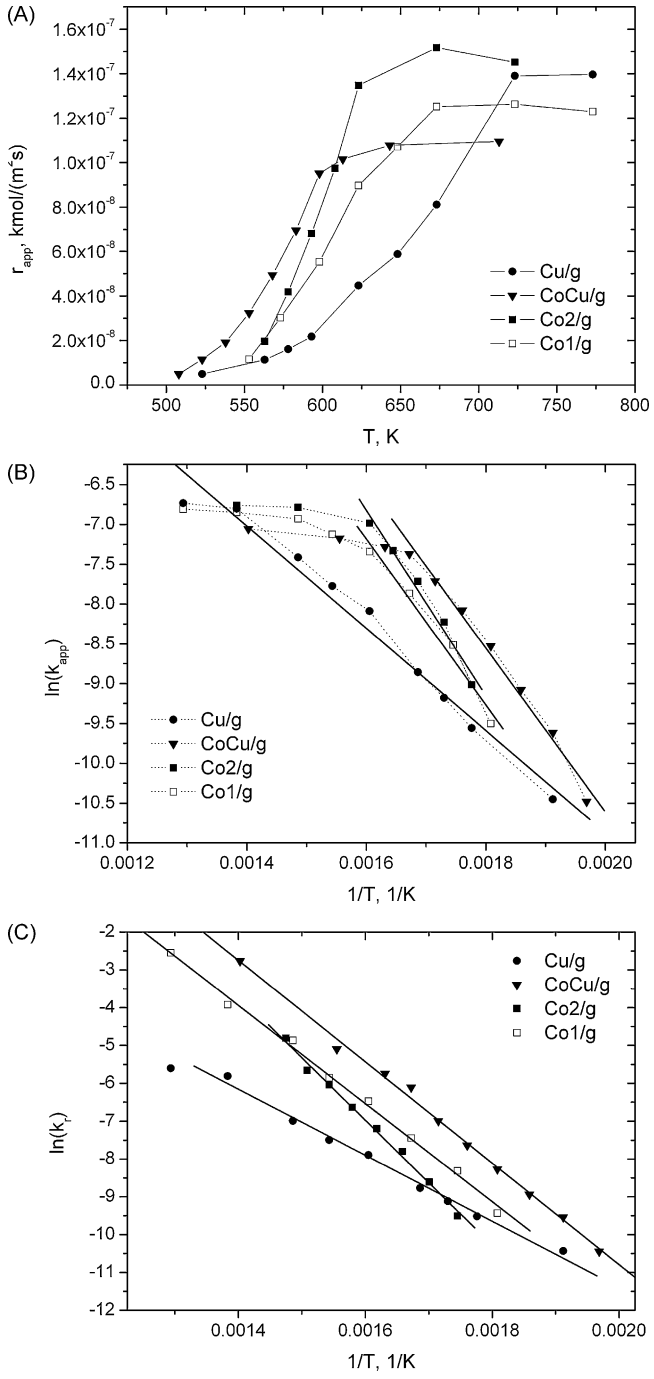

Fig. 1. Temperature screening of the catalyst deposited on the wire gauzes: (A) temperature dependence of the apparent reaction rate of *n*-hexane combustion, r_{app}; (B) Arrhenius plots for apparent rate constants, k_{app}; (C) Arrhenius plots for kinetic rate constants, k_r.

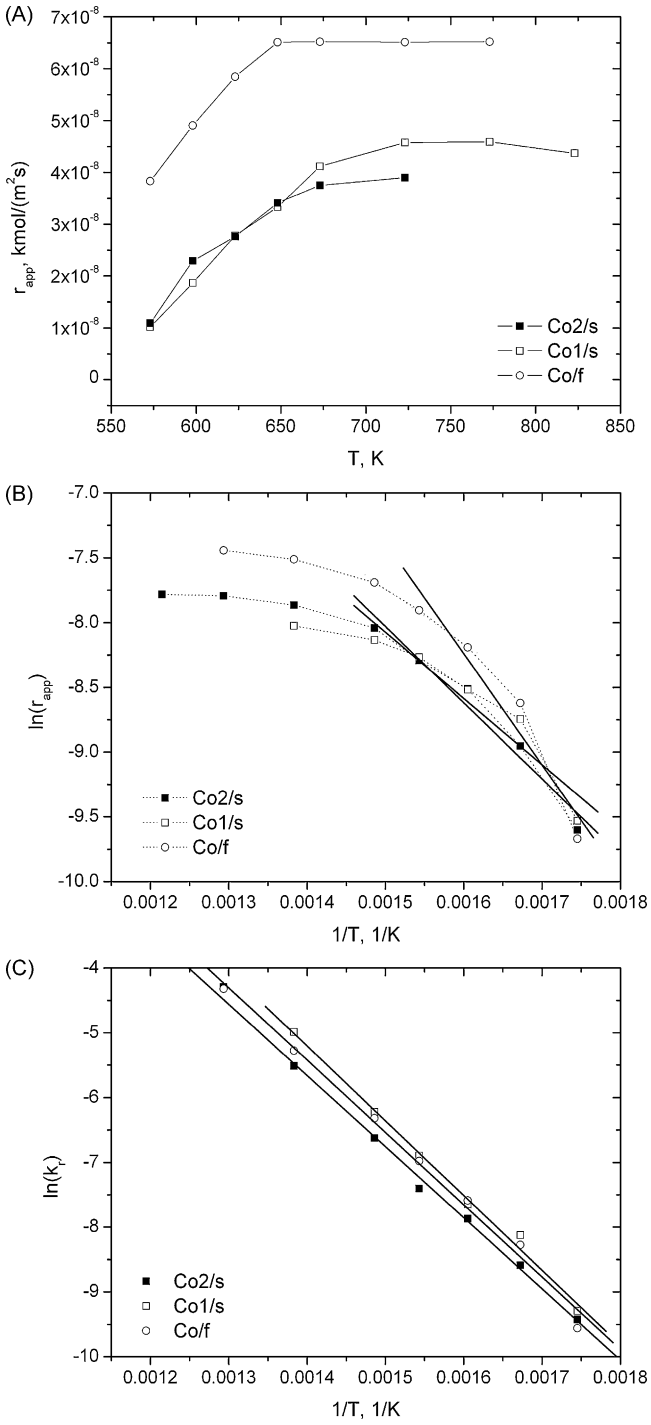

Fig. 2. Temperature screening of the catalyst deposited on the steel sheets: (A) temperature dependence of the apparent reaction rate of *n*-hexane combustion, r_{app}; (B) Arrhenius plots for apparent rate constants, k_{app}; (C) Arrhenius plots for kinetic rate constants, k_r.

mass transport exerted an effect on the values of the infinite apparent rate constant $k_{app,\infty}$ which are on the low side and bear quite large experimental error for all the samples and especially for those deposited on steel sheets (Fig. 2B). The same conclusion may concern the values of the apparent activation energy E_{app} which are much lower (around 30 kJ/mol) for the corresponding samples deposited on the steel sheets than on the wire gauzes. Our idea is then to provide a reliable approach to separate the mass transport from internal kinetics to obtain pure kinetic parameters and to check how this may improve the quality of their optimisation. The pure kinetic parameters are not only a measure of the intrinsic catalytic activity but also are necessary for the equation describing the whole reactor performance. For this reason their estimation has also a practical aspect connected with the reactor design.

3.1. Approach to mass transport separation

The mass transfer impact can be considered as two boundary cases:

- external transfer resistance at the catalyst external surface that could limit the overall process rate;

Table 2
The results of the optimisation of the kinetic and mass transport parameters obtained for *n*-hexane combustion in the CSTR type reactor.

Sample name	$k_{app,\infty}$ (m/s)	Relative error	E_{app} (kJ/mol)	Relative error	R^2	k_C (m/s)	$k_{r,\infty}$ (m/s)	Relative error	E_A (kJ/mol)	Relative error	R^2
Cu/g	7.15 ± 2.3	0.32	53.4 ± 3.2	0.06	0.976	17.6×10^{-4}	$4.39 \pm 0.37 \times 10^{2}$	0.09	72.6 ± 2.6	0.04	0.992
CoCu/g	$2.14 \pm 0.20 \times 10^{4}$	0.09	85.5 ± 4.2	0.05	0.988	8.75×10^{-4}	$9.25 \pm 0.30 \times 10^{6}$	0.03	111.5 ± 2.5	0.02	0.996
Co2/g	$1.34 \pm 0.19 \times 10^{5}$	0.14	96.8 ± 8.3	0.09	0.979	7.73×10^{-4}	$2.95 \pm 0.12 \times 10^{8}$	0.04	137.5 ± 4.1	0.03	0.995
Co1/g	$1.32 \pm 0.29 \times 10^{4}$	0.22	86.6 ± 10.2	0.12	0.973	11.2×10^{-4}	$1.54 \pm 0.06 \times 10^{6}$	0.04	107.9 ± 2.8	0.03	0.996
Co2/s	6.59 ± 4.8	0.73	54.3 ± 7.0	0.13	0.976	6.12×10^{-4}	$1.65 \pm 0.06 \times 10^{4}$	0.04	91.2 ± 2.0	0.02	0.997
Co1/s	3.07 ± 5.7	1.84	50.1 ± 10.4	0.21	0.920	5.10×10^{-4}	$5.68 \pm 0.37 \times 10^{4}$	0.07	95.9 ± 3.8	0.04	0.994
Co/f	$2.46 \pm 1.2 \times 10^{2}$	0.49	71.4 ± 13.6	0.19	0.932	4.25×10^{-4}	$2.74 \pm 0.18 \times 10^{4}$	0.07	92.8 ± 3.7	0.04	0.992

- internal resistance due to the diffusion of the reactants in the pores of catalytic grain or layer.

Since the catalyst layers deposited by NEP are thin and non-porous we can neglect internal mass transfer.

For any solid catalyst the mass transfer has to be balanced by chemical reaction according to the formula:

$$k_C(C_A - C_{AS}) = k_r C_{AS} \tag{2}$$

here, k_C is mass transfer coefficient, m/s, k_r – intrinsic kinetic constant, m/s (first-order reaction assumed), C_A and C_{AS} are reactant A concentration, kmol/m^3, in the fluid and at the catalyst surface, respectively. After the re-arrangement:

$$C_{AS} = C_A \frac{k_C}{k_C + k_r} \tag{3}$$

The adjacent kinetic equation is as follows:

$$-r_A = k_{app} C_A = k_r C_{AS} = C_A \frac{k_r k_C}{k_C + k_r} = C_A \frac{1}{1/k_C + 1/k_r} \tag{4}$$

The intrinsic kinetic constant k_r refers to the concentration C_{AS} at the catalytic surface while the apparent constant k_{app} concerns the gas phase concentration. The equation distinctly shows that the observed kinetics is influenced either by the "mass transfer resistance" ($1/k_C$) or the "reaction resistance" ($1/k_r$). When the mass transfer is fast comparing to the reaction, we observe the intrinsic kinetics while in the opposite case – predominantly the mass transfer (C_{AS} approaching zero):

$$\begin{aligned} k_C >> k_r &: -r_A = k_r C_A \\ k_r >> k_C &: -r_A = k_C C_A \end{aligned} \tag{5}$$

For a given value of the observed apparent rate constant k_{app} we may determine mass transfer coefficient k_C and derive intrinsic kinetic constant k_r from Eq. (4):

$$k_r = \frac{k_{app} k_C}{k_C - k_{app}} \tag{6}$$

The problem becomes more complicated when we start to consider temperature dependence of the reaction rate govern by Arrhenius equation:

$$k_r = k_{r,\infty} \exp\left(\frac{-E_A}{RT}\right) \tag{7}$$

In general, the kinetic rate constant grows exponentially with temperature, while the mass transfer coefficient much less rapidly. To find the temperature dependence of k_C, a universal equation for packed beds can be applied according to Hobler [20]:

$$Sh = 0.11 Re^{0.8} Sc^{1/3} \tag{8}$$

or in a developed form:

$$\left(\frac{k_C d}{D_A}\right) = 0.11 \left(\frac{w d \rho}{\eta}\right)^{0.8} \left(\frac{\eta}{\rho D_A}\right)^{1/3} \tag{9}$$

This leads to a formula for the mass transfer coefficient:

$$k_C = 0.11 w^{0.8} d^{-0.2} \left(\frac{\rho}{\eta}\right)^{0.47} D_A^{2/3} \tag{10}$$

Temperature dependence of the diffusivity D_A can be regarded according to the Gilliland equation [20]:

$$\frac{D_A}{D_{A0}} = \left(\frac{T}{T_0}\right)^{3/2} \tag{11}$$

The equation of Sutherland [21] describes the temperature influence on the dynamic viscosity (constant 114 for air):

$$\eta = \eta_0 \frac{T_0 + 114}{T + 114} \left(\frac{T}{T_0}\right)^{3/2} \tag{12}$$

and the density is:

$$\rho = \rho_0 \frac{T_0}{T} \tag{13}$$

For certain cases (e.g. of the gradientless reactor) the velocity w can be assumed as constant; the same concerns the characteristic dimension d. After substituting temperature dependences (11)–(13) to Eq. (10) and collecting all the constants (including w, d, T_0, D_{A0}, η_0, ρ_0) in the single constant B, we can obtain approximate formula describing the dependence of mass transfer coefficient on temperature:

$$k_C = B\left[\left(T^{-2.5} \frac{T + 114}{T_0 + 114}\right)^{0.47} T\right] \cong B[0.106 T^{0.22}] \tag{14}$$

Since Eq. (14) shows that k_C weakly depends on temperature, in the first approach to the problem we may assume k_C as independent of temperature.

3.2. Data processing

The value of k_C is not known and it is rather difficult to be measured directly, however, it can be derived from the kinetic temperature experiments collected in the reactor. The procedure of the optimization of the parameters involves transformation of the coordinates from $k_{app}(T)$ to $k_r(T)$ using Eq. (6) and assuming $k_r(T)$ obeying Arrhenius Eq. (7). Thus the optimised k_C values correspond to the best linear regression found for the set of k_{app} at a given temperature. The k_C values found in this way for all the samples are included in Table 2. The results of the transformation of the coordinates are presented as Arrhenius plots in Figs. Fig.11C and Fig.22C. The fit of the Arrhenius equation to the transformed kinetic data gives the values of the kinetic parameters $k_{r,\infty}$ and E_A included in Table 2.

Taking into account the experimental error, the fitting statistics expressed by the correlation coefficient R^2 (Table 2) is very good. The kinetic parameters derived bear much less experimental error than their apparent counterparts from the original data (compare $k_{app,\infty}$ with $k_{r,\infty}$ and E_{app} with E_A and their relative errors in

Table 2). Another validation of the procedure, except the relative errors estimation, is that the Arrhenius plots of k_r obtained for the Co catalysts on the steel sheets and the one obtained from pure Co foil nearly coincide (Fig. 2C).

3.3. Catalysts evaluation

As can be seen from the comparison of the values of the apparent and intrinsic activation energ,y mass trasport has a profound effect on the kinetic parameters derived (Table 2). Since mass transport supressess the reaction rate it also causes the underestimation of the observed activation energy. We may thus treat the proposed method of the extraction of the mass transfer as some sort of the self-consistent approach which bases on the maximum optimised value of activation energy. In this way the observed activation energy can be treated as an estimator of the mass transport resistance during the reaction.

The values of the transport coefficients derived in the modelling section are rather small and much lower than infinite rate constants $k_{r,\infty}$ indicating a profound impact of the mass transport resistance on the overall reaction rate especially at higher temperature. As could be expected the mass transfer coefficients for the wire gauze samples are 2–3 times higher than for the steel sheets, but the difference is rather moderate judging by high mass transfer intensity of the gauzes determined independently [1,3]. Although the k_C values for each class of the samples (gauzes and sheets) are close to each other, some deviations are visible. Possible reason for that can be a certain impact of the sample orientation in the reactor basket. Some elements of the reactor can also screen the sample decreasing mass transfer rate. The overall conclusion is that the stirred jet reactor does not give the sufficient mixing condions and does not apply for the determination of the intrinsic kinetic parameters, which can be obtained anyway through modelling the reactor.

The values of activation energy obtained for the cobalt catalysts (110 kJ/mol on average) are on average higher than those reported in the literature for a similar systems with cobalt oxide catalysts [22,23]. This again puts forward a question of the impact of mass transport on the observed kinetics and the necessity of elaborating the methods which would secure lab-to-lab congruence of the kinetic parameters. The values derived for the wire gauze sample are by around 20 kJ/mol higher than for the sheet samples which may suggest that mass transport still contributes to the latter. The highest activation energy (137 kJ/mol) was noted for the most loaded cobalt catalyst (Co2/g) on the gauze repeated also for other analogous samples not shown in this paper which may indicate on the structure sensitivity of combustion. Finally, in the series of the catalyst Co/g, CoCu/g, Cu/g a decreasing tendency in the values of activation energy may reflects growing contribution of the more active catalyst.

The estimated values of the infinite rate constants are sensitive more to the carrier structure rather than the catalyst composition: they are by 2–4 orders of magnitude higher for the gauze catalysts (except Cu/g) than for those on the sheets. This indicates that the gauze open structure allows for much higher velosities (the unit of $k_{r,\infty}$ is m/s) of the gas molecules. The low value etimated for the Cu/g sample may be due to the high error and the lowest correlation coefficient of fitting obtained for it as it can be inferred from the data in Table 2.

The copper doped cobalt catalyst deposited on wire gauze (CoCu/g) beats the other catalyst in terms of the overall reaction rate and the initiation temperature (Fig. 1A). For this sample the reaction ignition was at around 220 °C while for the other cobalt catalysts at around 280 °C. As demonstrated for the Cu reference sample copper apparently facilitates low temperature combustion of hexane.

4. Conclusions

The paper deals with the evaluation of the cobalt and copper doped cobalt catalysts deposited on the structured steel carriers (wire gauzes, reference sheets) with low temperature plasma technique which has been adapted by us for the catalyst layering, The wire gauze carriers are regarded here as fillers of the converter for VOC combustion.

Our idea was to compare the catalysts performance in terms of their light-off temperature and the kinetic parameters (infinite rate constant, activation energy). However, the analysis of the kinetic results showed a huge impact of the external mass transfer on the observed reaction rate, which was still present in the jet-stirred reactor used for the kinetic study. It caused a substantial underestimation of both parameters. The proposed reactor model and its optimization allowed to extract mass transport coefficient from the apparent rate constants to obtain the intrinsic kinetic constants, which were further used for the evaluation of the catalysts.

Among the studied catalysts the best performance was noted for the copper doped cobalt catalyst deposited on the wire gauzes as it demonstrated the highest rate of *n*-hexane combustion and the lowest reaction initiation temperature (220 °C) with comparable activation energy (111 kJ/mol) and infinite rate constant (9.25×10^6 m/s). The values obtained by us are higher than those reported in the literature for the similar systems. The wire gauze carriers again confirmed much better mass transfer coefficients than the reference carriers in form of sheets.

Acknowledgements

The study was partly supported by the Polish State Committee for Scientific Research which funded the project N209144736 (2009–2012). The financial support is gratefully acknowledged.

References

[1] A. Kołodziej, J. Łojewska, Top. Catal. 42 (2007) 475–480.
[2] A. Kołodziej, J. Łojewska, Catal. Today 105 (2005) 378–384.
[3] J. Łojewska, A. Kołodziej, R. Kapica, T. Łojewski, J. Tyczkowski, Catal. Commun. 10 (2009) 142–145.
[4] A.F. Ahlström-Silversand, C.U.I. Odenbrand, Chem. Eng. J. 73 (1999) 205–216.
[5] G. Ertl, H. Knözinger, F. Schüth, J. Weitkamp (Eds.), Handbook of Heterogeneous Catalysis, Wiley-VCH, 2008.
[6] G. Busca, M. Daturi, E. Finocchio, V. Lorenzelli, G. Ramis, R.J. Willey, Catal. Today 33 (1997) 239–249.
[7] B. Solsona, T.E. Davies, T. Garcia, I. Vazquez, A. Dejoz, S.H. Taylor, Appl. Catal. B 84 (2008) 176–184.
[8] U. Zavyalova, B. Nigrovski, K. Pollok, F. Langenhorst, B. Müller, P. Scholz, B. Ondruschka, Appl. Catal. B 83 (2008) 221–228.
[9] P.A. Neeft, M. Makkee, J.A. Moulijn, Appl. Catal. B: Environ. 8 (1996) 57–78.
[10] J.P.A. Neeft, O.P.P. van Pruissen, M. Makkee, J.A. Moulijn, Appl. Catal. B: Environ. 12 (1997) 21–31.
[11] P.G. Harrison, I.K. Ball, W. Daniell, P. Lukinskas, M. Céspedes, E.E. Miró, M.A. Ulla, Chem. Eng. J. 95 (2003) 47–55.
[12] G.R. Castro, J. Küppers, Surf. Sci. 123 (1982) 456–470.
[13] A. Bogen, J. Küppers, Surf. Sci. 134 (1983) 223–226.
[14] L.F. Liotta, G. Di Carlo, G. Pantaleo, A.M. Venezia, G. Deganello, Appl. Catal. B: Environ. 66 (2006) 217.
[15] J. Tyczkowski, R. Kapica, J. Łojewska, Thin Solid Films 5/16 (2007) 6590–6595.
[16] J. Łojewska, A. Kołodziej, P. Dynarowicz-Łątka, A. Wesełucha-Birczyńska, Catal. Today 101 (2005) 81–91.
[17] J. Łojewska, A. Kołodziej, J. Żak, J. Stoch, Catal. Today 105 (2005) 655–661.
[18] J. Łojewska, P. Dynarowicz-Łątka, A. Kołodziej, Thin Solid Films 495 (2006) 299–307.
[19] http://www.autoclaveengineers.com/products/catalytic_reactors/micro_berty/.
[20] T. Hobler, Diffusive mass transport and absorbers (Dyfuzyjny ruch masy i absorbery), WNT Warszawa, 1976.
[21] T. Hobler, Ruch ciepła i wymienniki (Heat transport and exchangers), WNT Warszawa, 1979.
[22] V.R. Choudhary, S. Banerjee, S.G. Pataskar, Appl. Catal. A: Gen. 253 (2003) 65–74.
[23] N. Bahlawane, Appl. Catal. B: Environ. 67 (2006) 168–176.